

## Mössbauer measurements in iron-base alloys with nontransition elements\*

I. Vincze

Central Research Institute for Physics, H 1525 Budapest, P.O.B. 49, Hungary

A. T. Aldred

Argonne National Laboratory, Argonne, Illinois 60439

(Received 18 September 1973)

The hyperfine field and isomer shift at iron sites in dilute iron-base alloys containing Ge, As, Sn, and Sb impurities were determined by Mössbauer measurements. Similar information was obtained for the tin sites in FeSn alloys. These experimental data, together with those published earlier for Al, Si, and Ga solutes, support a model which supposes that only the impurity excess  $p$  electrons take part in the charge screening. The interactions between iron spin-up  $3d$  electrons and impurity  $4s^2$  or  $5s^2$  electrons are held responsible for the increase in iron moment with impurity concentration in the case of Ga, Ge, As, Sn, and Sb solutes.

### I. INTRODUCTION

Nontransition elements dissolved in a ferromagnetic matrix such as iron are expected to be nonmagnetic because the  $d$  electrons at the nontransition-element sites are either nonexistent (e.g., Al and Si) or are in fully occupied energy levels (e.g., Ga, Ge, As, Sn, and Sb). This expectation was confirmed by the neutron scattering measurements of Holden *et al.*,<sup>1</sup> which showed that these solutes (no measurements were performed for FeAs) do not carry any well-localized moments within the experimental error of  $\pm 0.5\mu_B$ . However, Holden *et al.* found that in the alloys in which the solutes had fully occupied  $d$  levels, the iron atoms within 4–5 Å of an impurity had moments which were increased by  $\sim 1$ –2% over the value for pure iron. This effect is also evident in the concentration dependence of the bulk magnetization,  $d\bar{\mu}/dc$ . Thus, Al and Si impurities (without  $d$  electrons) result in simple dilution<sup>2</sup> ( $d\bar{\mu}/dc = -2.2\mu_B/\text{atom}$ ), whereas those solutes with fully occupied  $d$  levels cause deviations from simple dilution that are independent of the outer-electron configuration. For Ga, Ge, and As impurities<sup>3,4</sup> (with filled  $3d$  shells),  $d\bar{\mu}/dc = -1.4\mu_B/\text{atom}$ , and for Sn and Sb impurities<sup>4</sup> (with filled  $4d$  shells),  $d\bar{\mu}/dc = -0.97\mu_B/\text{atom}$ . On the other hand, Cu and Zn impurities, despite their filled  $3d$  shell, give  $d\bar{\mu}/dc = -2.0\mu_B$ .<sup>4,5</sup>

It appears that these features of the iron-magnetic-moment disturbance are connected with the charge screening of the impurity valence electrons. Originally, it was thought that the excess electrons enter into the  $d$  band of iron,<sup>6</sup> but specific-heat measurements<sup>7</sup> have ruled out this possibility. The substantially unchanged electronic specific heat with alloying also invalidates the argument that the effect of the impurity is to shift the spin-up and spin-down half-bands with respect to each other and thereby cause an increase in the iron moment.

Another suggestion<sup>3,4</sup> attributes the increase in iron moment to a decrease in the antiparallel (to the  $3d$  moment)  $4s$  moment. Indeed, if the screening of the impurity excess charge takes place in the  $4s$  conduction band of iron, then the attractive impurity potential will reduce the  $4s$ -electron density at the neighboring iron sites. If the net iron-conduction-electron polarization is negative<sup>8</sup> (although the evidence is not clear-cut),<sup>9</sup> this decrease in the number of conduction electrons at the iron sites would lead to an increase in the iron moment. The main difficulty with this suggestion is that the charge screening should depend strongly on the excess charge. Thus we should expect different  $d\bar{\mu}/dc$  values for the different columns in the Periodic Table, rather than for the different periods, as observed.<sup>3,4</sup>

The Mössbauer effect is a useful tool for the investigation of the impurity-charge-screening mechanism, because the hyperfine field and the isomer shift are sensitive to changes in the  $d$ - and  $s$ -electron spin and the charge densities, respectively. Although many Mössbauer investigations have been reported on iron-base alloys with nontransition elements (predominantly with Al and Si), the published data<sup>10–20</sup> do not give a uniform picture of the charge-screening process. The results of <sup>57</sup>Fe Mössbauer measurements on iron-base alloys containing Ge, As, Sn, and Sb impurities are reported in the present paper, together with results of <sup>119</sup>Sn measurements on FeSn alloys. After the experimental details are given, the results are compared with the models mentioned above and a slightly different model is proposed.

### II. EXPERIMENTAL METHOD AND RESULTS

#### A. Apparatus

A conventional constant-acceleration Mössbauer spectrometer was used<sup>20</sup> with a 1024-channel NTA 512-B analyzer. The differential nonlinearity

proved to be better than 0.1%, and no measurable change of velocity or zero point could be observed even during runs over several days. For the iron spectra, 10- and 50-mCi  $^{57}\text{Co}$  sources diffused in chromium were used, whereas the  $^{119}\text{Sn}$  measurements utilized a 5-mCi  $\text{BaSnO}_3$  source. The liquid-nitrogen-temperature measurements on  $^{119}\text{Sn}$  were performed with a "cold-finger" cryostat. Each iron spectrum was taken with  $300\text{--}500 \times 10^3$  counts per channel, and each tin spectrum was taken  $1\text{--}2 \times 10^6$  counts per channel; both were collected over a two-day run. The depth of the outer lines in the spectra is about  $40\text{--}60 \times 10^3$  counts per channel.

### B. Samples

The same alloys prepared for earlier magnetization measurements<sup>3,4</sup> were used. Only three  $\text{FeGe}$  samples could be rolled; all others were too brittle. Therefore, for the Mössbauer measurements, powder specimens with a grain size  $< 50 \mu\text{m}$  were filed from the ingots. The parameters obtained from powder and plate-form samples were the same within experimental error. All the alloys were disordered, and except for two  $\text{FeSb}$  alloys, they were single phase. In the  $\text{Fe-4.2-at.}\% \text{-Sb}$  and  $\text{Fe-4.4-at.}\% \text{-Sb}$  samples, a second phase was observed (about 8–10% of the iron present), which

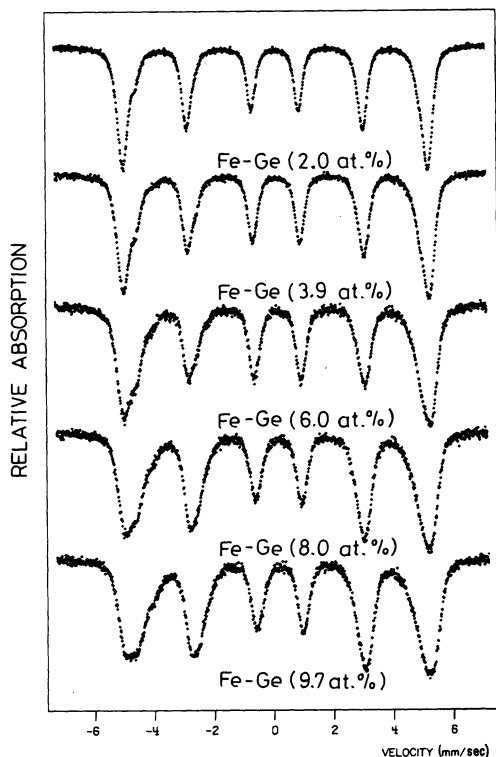


FIG. 1. Room-temperature Mössbauer spectra of  $\text{FeGe}$  alloys.

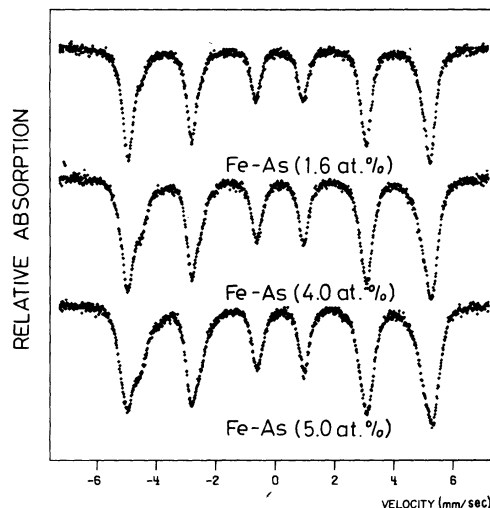


FIG. 2. Room-temperature Mössbauer spectra of  $\text{FeAs}$  alloys.

gave a broad paramagnetic line in the Mössbauer spectra at room temperature. The isomer shift of the second phase,  $+0.51 \pm 0.02 \text{ mm/sec}$  with respect to pure iron, corresponds to that of iron-rich  $\text{FeSb}$ ,<sup>21</sup> and the appearance of this phase was probably caused by the filing operation.

Although the original alloys were heat treated to ensure maximum homogeneity, the difficulty in preparing some of the ingots (because of the volatility of the nontransition element), combined with the fact that the samples had been sitting in a metastable condition for several years at room temperature, could lead to discrepancies between the original, chemically-analyzed concentrations and those determined in the fit. In fact, the impurity concentrations of the alloys determined from the Mössbauer spectra agreed well with the values given in the earlier papers<sup>3,4</sup> for most of the alloys; significant deviations were found for several samples as will be noted in Sec. IC. It is anticipated that the compositions determined from the spectra are the correct ones for the particular samples.

### C. Evaluation of the data

#### 1. Iron spectra

The iron spectra taken at room temperature are shown in Figs. 1–4. On each spectrum, we have performed three types of evaluation with different primary assumptions:

Type I: Only the first-neighbor effects are resolvable in the Mössbauer spectra.

Type II: Only the first- and second-neighbor effects are resolvable.

Type III: The second-neighbor effects are unresolvable and we can determine only the first- and third-neighbor effects.

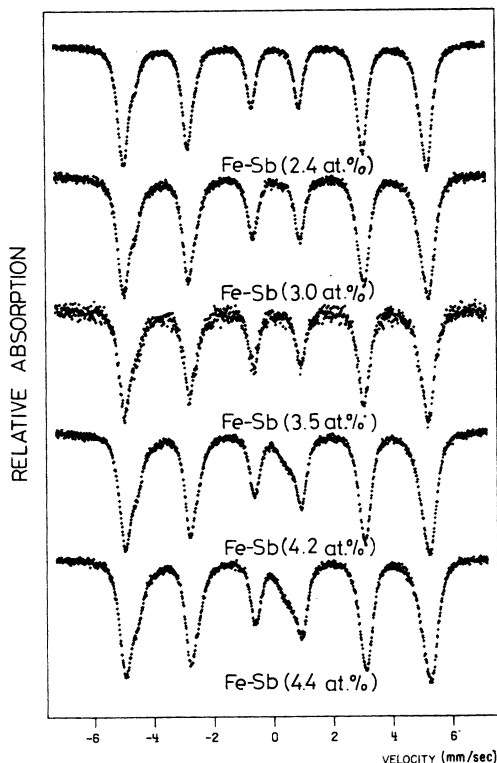


FIG. 3. Room-temperature Mössbauer spectra of FeSb alloys.

In addition to the above, the following assumptions<sup>22</sup> were used: (a) the line shape is Lorentzian, (b) the linewidth is an iteration parameter, and (c) the multiple impurity-neighbor effects are additive, i. e.,

$$H(n, m) = H_0 + n\Delta H_1 + m\Delta H_{2,3}$$

for the hyperfine field, and

$$i(n, m) = i_0 + n\Delta i_1 + m\Delta i_{2,3}$$

for the isomer shift. Here  $\Delta H_1$ ,  $\Delta H_{2,3}$  and  $\Delta i_1$ ,  $\Delta i_{2,3}$  are the changes of the hyperfine field and isomer shift in the first coordination shell and the second or third coordination shell due to the impurity, whereas  $H_0$  and  $i_0$  are the parameters of the central line;  $n$  and  $m$  are the numbers of impurities in the first shell and the second or third shell, respectively. The relative amplitude of the six-line patterns corresponding to iron atoms in a given configuration was assumed to be given by the binomial distribution, where the impurity concentration was considered to be an iteration parameter. In this manner the impurity concentration was evaluated from the observed satellite intensities.

The quality of the fit of the data to the theoretical curve was tested by computing the  $\chi^2$  value, defined in the usual way, and the effect of the introduction

of a new parameter or a new assumption on the value of  $\chi^2$  was investigated. It is clear that the type-I decomposition serves as a basis for comparison. The type-II evaluation is widely used for the decomposition of Mössbauer spectra,<sup>10,12,14-18</sup> but no direct evidence exists to justify this procedure. Moreover, NMR measurements<sup>23-25</sup> on FeAl alloys clearly show that the hyperfine-field change caused by the third-neighbor impurity is more important than that of the second-neighbor impurity. A similar conclusion was made for FeSi alloys from Mössbauer measurements on a single crystal.<sup>13</sup> This has motivated the type-III decomposition, but it should be mentioned that, in the case of FeSn alloys, a  $\Delta H_3 = +3.0$  kOe contribution was measured<sup>26</sup> by the continuous-wave NMR method, which is of opposite sign to the present result.

All the alloys showed similar behavior for the three decompositions. Evaluations II and III gave equally good fits, which means that the values of  $\chi^2/\langle\chi^2\rangle$ , where  $\langle\chi^2\rangle$  is the expected value of  $\chi^2$ , were the same within the standard deviation of  $\chi^2$ , about 0.06. On the scale of Figs. 1-4, it would not be possible to draw two separate curves distinguishing between evaluations II and III. The values of  $\Delta H_1$  and  $\Delta i_1$  for evaluations I-III were the same within experimental error. Similarly,  $d\bar{H}/dc$  and  $d\bar{i}/dc$ , the average change of the hyperfine field and the isomer shift with concentration, respectively, are independent of the decomposition methods, although the values of  $H_0$ ,  $i_0$ ,  $\Delta H_2$ ,  $\Delta i_2$ , and

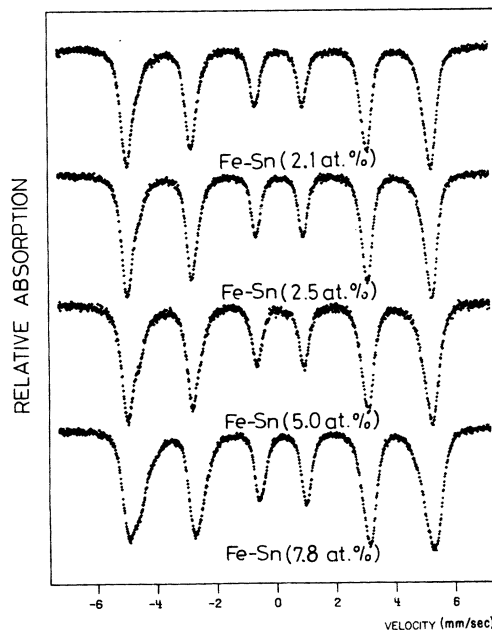


FIG. 4. Room-temperature iron Mössbauer spectra of FeSn alloys.

TABLE I. Parameters evaluated for the Fe-5.0-at.-%-Sn alloy using different assumptions in the decomposition. The assumptions in the evaluations and the meaning of the parameters are explained in the text.

Type of decomposition	$\Delta H_1$ (kOe)	$\Delta H_2$ or $\Delta H_3$ (kOe)	$\Delta i_1$ (mm/sec)	$\Delta i_2$ or $\Delta i_3$ (mm/sec)	$d\bar{H}/dc$ (kOe)	$d\bar{i}/dc$ (mm/sec)	$X^2/\langle X^2 \rangle$
I	-22.8(3) <sup>a</sup>		0.044(3)		-150(7)	+1.35(5)	3.67
II	-22.1(3)	-13.6(5)	0.051(4)	-0.001(6)	-160(7)	+1.38(9)	2.18
III	-22.6(3)	-11.0(3)	0.055(3)	-0.006(4)	-175(10)	+1.41(10)	2.11
IV	-22.6(3)	-13.5(3)	0.055(3)	-0.004(4)	-165(9)	+1.40(9)	1.95

<sup>a</sup>Values in parentheses represent statistical uncertainties in the final significant figures.

$\Delta H_3$ ,  $\Delta i_3$  are obviously different. In each case the decomposed value of the linewidth was larger than that for pure iron. As a typical example, the data for the Fe-5.0-at.-%-Sn alloy are presented in Table I. Also included are the results of a tenta-

tive decomposition, denoted by IV, in which the Sn third-neighbor effect was fixed at the value given by the NMR experiment,<sup>26</sup> and a fit was made for the first- and second-neighbor effects. Again, the change in  $\chi^2/\langle \chi^2 \rangle$  is not significant.

TABLE II. Change of the hyperfine field  $\Delta H_1$  and isomer shift  $\Delta i_1$  at the first iron neighbors of an impurity, the total change of the isomer shift  $d\bar{i}/dc$ , and the hyperfine field at iron atoms with no first-neighbor impurities for the alloys listed. The concentrations labeled Mössbauer are those determined in the fit. The concentrations labeled chemical represent chemically analyzed concentrations ( $\pm 0.1$  at. %) given in previous papers (Refs. 3 and 4).

FeGe alloys					
Ge concentration (at. %)		$\Delta H_1$	$\Delta i_1$	$d\bar{i}/dc$	$H_0$
Mössbauer	Chemical	(kOe)	(mm/sec)	(mm/sec)	(kOe)
2.0(2)	2.0	-23.4(3)	0.059(4)	0.86(11)	330.3(2)
3.9(2)	3.9	-23.0(3)	0.052(3)	0.85(6)	331.5(2)
6.0(1)	6.0	-24.0(3)	0.047(3)	0.82(6)	332.8(2)
8.0(2)	8.0	-24.8(3)	0.046(3)	0.81(7)	334.7(3)
9.7(1)	9.7	-24.8(3)	0.043(3)	0.85(5)	336.6(4)
FeAs alloys					
As concentration (at. %)		$\Delta H_1$	$\Delta i_1$	$d\bar{i}/dc$	$H_0$
Mössbauer	Chemical	(kOe)	(mm/sec)	(mm/sec)	(kOe)
1.6(1)	2.2	-25.1(6)	0.079(6)	1.20(20)	330.8(2)
4.0(1)	4.0	-25.4(3)	0.070(4)	1.05(10)	331.1(2)
5.0(2)	5.9	-26.0(3)	0.066(4)	1.17(8)	334.4(2)
FeSn alloys					
Sn concentration (at. %)		$\Delta H_1$	$\Delta i_1$	$d\bar{i}/dc$	$H_0$
Mössbauer	Chemical	(kOe)	(mm/sec)	(mm/sec)	(kOe)
2.1(1)	2.1	-22.1(5)	0.057(5)	1.26(15)	330.1(2)
2.5(1)	4.0	-22.2(3)	0.059(5)	1.19(10)	330.5(3)
5.0(3)	5.7	-22.5(3)	0.050(4)	1.38(9)	331.5(2)
7.8(2)	7.8	-21.8(3)	0.042(3)	1.24(8)	334.1(2)
FeSb alloys					
Sb concentration (at. %)		$\Delta H_1$	$\Delta i_1$	$d\bar{i}/dc$	$H_0$
Mössbauer	Chemical	(kOe)	(mm/sec)	(mm/sec)	(kOe)
2.4(1)	1.6	-21.2(4)	0.073(5)	1.14(10)	330.9(2)
3.0(2)	3.0	-23.5(4)	0.060(5)	1.28(10)	331.7(2)
3.5(3)	3.9	-21.3(6)	0.070(6)	1.23(10)	331.7(3)
4.2(2)	4.2	-21.5(3)	0.066(4)	1.29(9)	332.6(2)
4.4(2)	6.5	-22.0(4)	0.060(5)	1.22(9)	333.0(2)

Summarizing the results, it can be seen that evaluations II and III are sensitive only to the asymmetric line broadening due to distant neighbors, and the values of  $\Delta H_2$  or  $\Delta H_3$  cannot be given any real physical meaning. The large line broadening (relative to the effect of  $3d$  impurities<sup>22</sup>) is probably connected with the charge-screening contribution to the change of hyperfine field, which has an  $r^{-2}$  dependence at large distances.<sup>27</sup> This observation agrees with the NMR experiments,<sup>26</sup> in which a similarly large line broadening was found for the third- and fourth-neighbor satellites for a tin impurity. Thus, it appears that only  $\Delta H_1$ ,  $\Delta i_1$ ,  $d\bar{H}/dc$ , and  $d\bar{i}/dc$  have any real physical meaning in the decomposed Mössbauer spectra.

In Table II we list the change of the iron hyperfine field ( $\Delta H_1$ ) and isomer shift ( $\Delta i_1$ ) due to a first-neighbor impurity, as well as the total change of the isomer shift with concentration ( $d\bar{i}/dc$ ) for each series of alloys, and it is apparent that they are each independent of the impurity concentration. On the other hand, the hyperfine field corresponding to the central line ( $H_0$ ) depends on the impurity concentration in a nonlinear manner (Table II).

### 2. Tin spectra

The room-temperature tin spectra of the  $FeSn$  alloys are shown in Fig. 5. They are reasonably well described by a highly broadened six-line pattern. The values of the average tin hyperfine field and isomer shift at room temperature determined

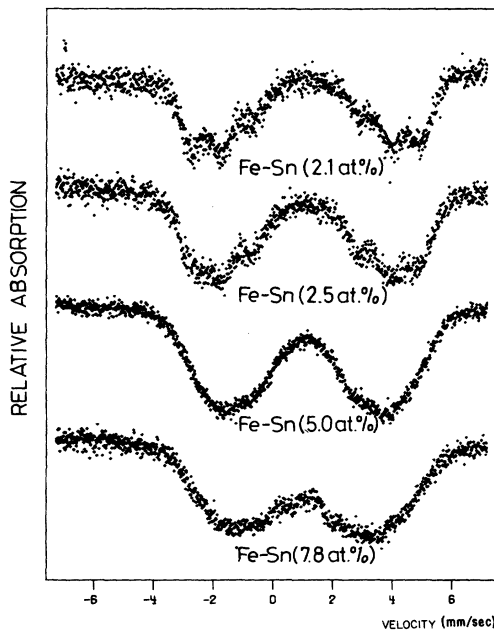


FIG. 5. Room-temperature tin Mössbauer spectra of  $FeSn$  alloys.

TABLE III. Absolute value of the average hyperfine field  $\bar{H}_{Sn}$ , the average isomer shift  $i_{Sn}$  (with respect to pure iron) at tin atoms, and the change of the tin hyperfine field due to a first-neighbor tin  $\Delta H_1$  for  $FeSn$  alloys at room temperature.

Sn concentration (at. %)	$\bar{H}_{Sn}$ (kOe)	$i_{Sn}$ (mm/sec)	$\Delta H_1$ (kOe)
2.1	75.0(6)	1.38(2)	-20.0(2.0)
2.5	71.9(4)	1.44(2)	-23.0(1.5)
5.0	63.6(4)	1.43(2)	-24.4(0.8)
7.8	55.7(5)	1.44(2)	-27.4(1.0)

from a six-line fit are presented in Table III. The absolute value of the average hyperfine field  $\bar{H}_{Sn}$  decreases rapidly as the tin concentration increases; at room temperature the data yield  $(d\bar{H}_{Sn}/dc) = -310 \pm 10$  kOe, and the tin hyperfine field extrapolated to zero tin concentration,  $H_{Sn}^0 = 79.4 \pm 0.8$  kOe. At liquid-nitrogen temperature,  $d\bar{H}_{Sn}/dc = -260 \pm 10$  kOe, and  $H_{Sn}^0 = 82.7 \pm 1.0$  kOe. This latter value agrees well with earlier direct measurements at low tin concentrations.<sup>28-30</sup> In the evaluation above, the tin nuclear-moment value in the excited state<sup>31</sup> was larger than that used in the previous evaluation.<sup>28</sup> The larger value of  $d\bar{H}_{Sn}/dc$  at room temperature relative to the 80 °K value may be attributed to the fact that, with an increase in temperature, the tin hyperfine field<sup>30</sup> decreases more rapidly than the iron hyperfine field. A similar linear fit of the average isomer shift against concentration gives  $d\bar{i}_{Sn}/dc = 0.9 \pm 0.5$  mm/sec and  $i_{Sn}^0 = 1.38 \pm 0.03$  mm/sec with respect to pure iron. This increase in isomer shift with an increase in tin concentration implies an increase in  $s$ -electron density at the tin nucleus.

The decomposed values of  $\Delta H_1$  shown in Table III are strongly dependent on the impurity concentration, and linear extrapolation to zero tin concentration gives  $\Delta H_1^0 = -19.2 \pm 1.0$  kOe. The line-widths obtained after the decomposition for the first-neighbor effect are much larger than that of the source linewidth. However, the larger line-width cannot be unambiguously attributed to unresolved distant-neighbor effects because the concentration dependence of  $\Delta H_1$  suggests a distribution of hyperfine fields, which may also lead to line broadening.

### D. Comparison of data-evaluation methods

One of the most interesting features of the present spectrum decomposition is that no impurity effects other than those of the first shell could be reliably determined. Before we compare the present with the previously reported data, it should be pointed out that the resolution of the spectra is at least four times better in the present experiments

than that obtained in earlier measurements. It would then appear that the results obtained by Stearns<sup>12</sup> from decomposed *FeAl* spectra, showing effects out to the fifth-neighbor shell (with half the present statistics), are questionable.

It was found previously<sup>22</sup> that an increase in statistics without any increase in the resolution of the spectra results in an increase in  $\chi^2/\langle\chi^2\rangle$ . Thus, the attempt to fit the spectra for *FeGa* alloys<sup>17</sup> with different six-line patterns corresponding to various first- and second-neighbor configurations introduce too many parameters. This is unjustified when a good fit can be obtained with less parameters.<sup>20</sup> The present parameters agree reasonably well with the reported values<sup>10,14</sup> for evaluation II. For example, in the case of *FeGe*, the average value of  $\Delta H_2$  (the change of the hyperfine field due to second-neighbor Ge) is  $-11.1$  kOe, which is in agreement with Ref. 14. On the other hand, significant deviations were observed in the case of *FeSb*,<sup>15</sup> probably because the composition is near the solubility limit. As was stressed in Ref. 22, the reason for the discrepancies between different Mössbauer results and between Mössbauer and various NMR data is the inadequate fitting procedure used in the analysis of the Mössbauer spectra.

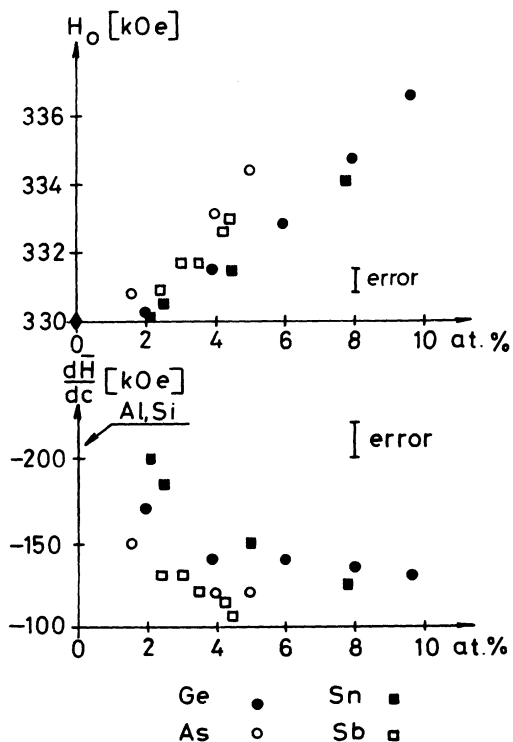


FIG. 6. Concentration dependence of the hyperfine field at iron atoms without first-neighbor impurities,  $H_0$ , and the total change of the average hyperfine field with concentration,  $d\bar{H}/dc$ . The figure contains earlier published data (Refs. 20 and 27) for Al and Si.

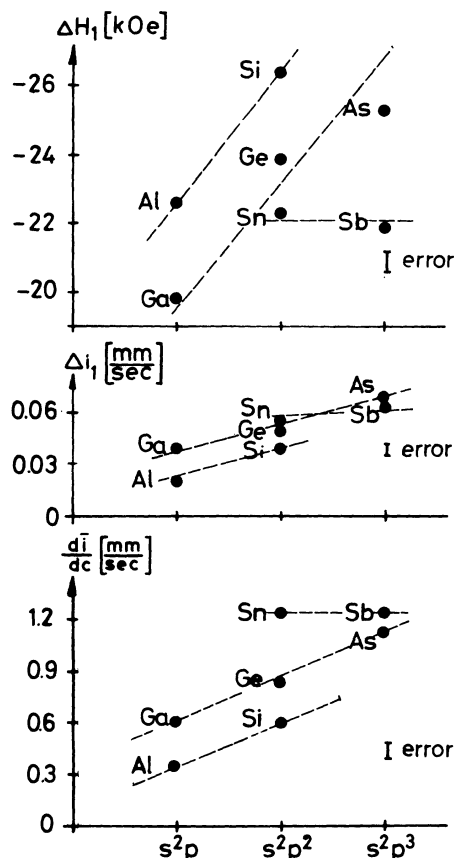


FIG. 7. Change of the hyperfine field,  $\Delta H_1$ , and isomer shift,  $\Delta i_1$ , at the first iron neighbors of the impurity and the total change of the isomer shift,  $d\bar{i}/dc$ , with concentration. The figure contains earlier published data (Refs. 20 and 27) for Al, Ga, and Si.

### III. DISCUSSION

The concentration dependence of the hyperfine field corresponding to the central line  $H_0$  is shown in Fig. 6. It was found for *FeAl* alloys<sup>20</sup> that  $dH_0/dc$  is constant, and the increase in  $H_0$  with  $c$  was attributed to the effect of unresolved satellites. Therefore, the deviation of  $H_0$  from linearity for the present alloys (Fig. 6) presumably reflects the increase in the average iron moment. A similar effect is observed in  $d\bar{H}/dc$  (Fig. 6).

The concentration dependences of  $\Delta H_1$ ,  $\Delta i_1$ , and  $d\bar{i}/dc$  for Ga, Ge, As, Sn, and Sb impurities in iron are given in Fig. 7; this figure also contains earlier data<sup>20,27</sup> for Al and Si impurities. In the case of the iron nucleus, the isomer shift reflects changes in the  $4s$  and  $3d$  populations; a positive change indicates a decrease in  $s$  or an increase in  $d$  occupation. For the tin nucleus, an increase in the isomer shift means an increase in the  $5s$  electron density.

Let us recapitulate briefly the results<sup>23</sup> concern-

ing the effect of solutes that do not contain occupied  $d$  levels (Al and Si). The perturbation of the isomer shift at iron sites reflects the screening of the impurity excess charge. The excess charge of Si, which is larger than that of Al, causes a greater increase in the changes of both the first-neighbor effect and the total isomer shift. Similarly, the change in the hyperfine field due to a first-neighbor Si impurity (including the contributions from the removed conduction-electron polarization and from charge screening) has a larger absolute value than the change due to an Al impurity because of the larger excess charge of Si. These observations, especially the isomer-shift results, are inconsistent with the theory<sup>32</sup> that the difference in behavior between Al and Si is due to an overlap effect. In fact, Al enlarges, whereas Si contracts, the iron lattice.<sup>33</sup>

Comparing the perturbations caused by Al and Si solutes with those caused by Ga and Ge, which have the same outer  $sp$  configurations over a full  $3d$  shell, it is found that the parameters show the same tendencies for both types of solutes. The  $\Delta H_1$ ,  $\Delta i_1$ , and  $d\bar{i}/dc$  values show nearly parallel trends for the same outer-electron configurations (Fig. 7). Thus the increase in these parameters with an increase in the number of outer electrons in the order Ga, Ge, and As can also be attributed to the charge-screening effect of the impurity valence electrons.

The strong dependence of  $d\bar{i}/dc$  on the number of excess electrons excludes the possibility that the observed values of  $d\bar{\mu}/dc$  reflect a decrease in the number of antiparallel  $4s$  electrons with an increase in solute concentration as a result of charge screening. Moreover, it should be noted that the contribution from the antiparallel  $4s$  moment to the increase in iron moment must be small because no difference is apparent between the effects of Ga, Ge, and As.

The increase in the iron moment is reflected in the spacing of the two nearly parallel lines for  $\Delta H_1$ ,  $\Delta i_1$ , and  $d\bar{i}/dc$  for the solutes with and without filled  $3d$  shells. If the decrease of about 2.5 kOe in the absolute value of  $\Delta H_1$  for Ga and Ge is attributed to the increased core-polarization contribution from the increased  $3d$  moment of the first iron neighbors, then the decrease corresponds to an increase of about  $0.05\mu_B$  when a core-polarization constant of  $50 \text{ kOe}/\mu_B$  is applied.<sup>34</sup> The relatively small change of  $\Delta H_1$  again rules out any  $4s$  contribution to the moment perturbation, because a much larger (about one order of magnitude) polarization constant is expected for the  $4s$  electrons. The increase of about 0.02 mm/sec in  $\Delta i_1$  for Ga and Ge, when compared with Al with Si, again suggests an increase in the iron  $d$ -electron density of about 0.05 electrons when the calibration of Danon<sup>35</sup>

is used (an increase of about 0.4 mm/sec in the isomer shift is produced by the addition of one more  $d$  electron if the  $4s$ -electron configuration is unchanged). Because the  $s$  electrons have at least twice as large an effect on the isomer shift as the  $d$  electrons, the observed difference in  $\Delta i_1$  on going from Al and Si to Ga and Ge again would correspond to a decrease in the  $4s$ -electron density that is too small to explain the observed increase in the iron moment. The same is true for the difference in  $d\bar{i}/dc$ .

The above data comparisons show that the increase in iron moment caused by the Ga-type impurities cannot be explained by a decrease in the antiparallel  $4s$  moment. A considerable  $4s$ -electron density perturbation due to Ga-type impurities is observed, which is not apparently connected to a similar  $4s$ -moment disturbance. At the same time an increase in  $3d$ -electron and spin density takes place. Half the total increase in iron moment apparently arises from the effects of impurity first neighbor.

The results from impurities with occupied  $4d$  shells (Sn and Sb) agree essentially with the above conclusions, but some differences are evident. The values of  $\Delta H_1$ ,  $\Delta i_1$ , and  $d\bar{i}/dc$  show a tendency to saturation. This tendency seems to be consistent with the different radial distributions of the iron-moment perturbation for these impurities (as compared with those of the filled  $3d$ -shell impurities) observed in the neutron-diffraction experiments.<sup>1</sup> All the  $\Delta H_1$  and  $d\bar{i}/dc$  suggest a somewhat larger iron-moment increase than for the solutes with occupied  $3d$  shells, which is in agreement with the larger values of  $d\bar{\mu}/dc$ .

The hyperfine properties observed at the tin sites yield additional information about the FeSn alloys. The most remarkable result is the extremely rapid decrease in the tin hyperfine field as the tin concentration increases. Indeed, the value of  $d\bar{H}_{\text{Sn}}/dc$  is several times larger than the full tin hyperfine field, which is thought to come entirely from conduction-electron polarization. The assumption of a strongly distance-dependent conduction-electron polarization at the tin sites can explain the rapid decrease found in the tin hyperfine field. This assumption seems to be justified by the large increase in the absolute value of the tin hyperfine field with pressure<sup>29</sup> and by its rapid decrease as the temperature increases.<sup>30,36</sup> The contribution to  $d\bar{H}_{\text{Sn}}/dc$  from the change in lattice dimensions with increasing tin concentration is estimated to be about -200 kOe, which together with the first-neighbor changes (about -150 kOe), can account for all the observed decrease. This estimate should be treated cautiously because of the absence of data on local lattice distortions and local compressibility. In the present estimate, the compressibility of pure iron<sup>37</sup> and

the average increase in the lattice parameter<sup>33</sup> with alloying were used in the transformation of the pressure dependence of the tin hyperfine field.<sup>29</sup> It is obvious that this description is formally equivalent to the assumption of a positive contribution<sup>32</sup> to the negative tin hyperfine field originating from misfit effects. However, the hyperfine-field systematics<sup>36</sup> and tin hyperfine-field data in Heusler alloys<sup>39</sup> make it unnecessary to introduce such a positive contribution that increases for larger volumes. The large decrease in  $\bar{H}_{\text{Sn}}$  precludes the existence of an antiparallel tin moment<sup>36</sup> arising from 3d-5s overlap, inasmuch as the disappearance of this positive contribution with increasing tin concentration would result in a much smaller change in  $\bar{H}_{\text{Sn}}$ .

It should be emphasized at this point that the charge screening and the moment perturbation caused by these nontransition impurities are quite different from those observed for the transition-metal impurities. For example, if the relations used to describe the effect of transition-metal solutes<sup>22</sup> were valid for these nontransition solutes, the values of  $d\bar{H}/dc$  would be nearly zero for Sn and Sb, which is in disagreement with the observed values.

We now present a simple model that will account for the above features of the impurity charge screening. It is an extension of the model proposed for FeAl alloys,<sup>40</sup> which in turn is based on one suggested by Marshall and published by Mott.<sup>41</sup> The

model supposes that the 3s<sup>2</sup> levels in aluminum and silicon (and the corresponding 4s<sup>2</sup> levels in Ga, Ge, and As, and 5s<sup>2</sup> levels in Sn and Sb) are, to a first approximation, well localized and lie below the 3d states of iron; then only the impurity excess charge caused by the p electrons is screened by the iron conduction electrons. This charge screening is responsible for the large observed isomer-shift perturbations, but, because of the small conduction-electron polarization, little or no perturbation of the iron moment occurs. Because the 3s<sup>2</sup> levels of Al and Si are well below the 3d levels of iron, no interaction takes place, and the iron moment is unchanged with alloying. However, it is expected that the 4s<sup>2</sup> levels in Ga, Ge, and As and the 5s<sup>2</sup> levels in Sb and Sn would be higher than the corresponding 3s<sup>2</sup> level, and, therefore, the chances of interaction with the 3d levels of iron (resulting in an increase in iron moment) would be greater. The overlap of the 5s<sup>2</sup> electrons with the iron d electron is greater than the corresponding 4s<sup>2</sup> overlap, and this suggests a larger moment increase for the former, which is in agreement with the experimental data. The model does not require the filled impurity d shells to participate in the increase in iron moment. The values of  $d\bar{\mu}/dc$  for Cu and Zn, which are near simple dilution can also be explained. Inasmuch as neither Cu nor Zn has a full 4s<sup>2</sup> shell, no localized level can be formed and no interaction with the iron d electrons is expected.

\*Work performed in part under the auspices of the U. S. Atomic Energy Commission.

<sup>1</sup>T. M. Holden, J. B. Comly, and G. G. Low, Proc. Phys. Soc. Lond. **92**, 726 (1967).

<sup>2</sup>M. Fallot, Ann. Phys. (Paris) **6**, 305 (1936); D. Parsons, W. Sucksmith, and J. W. Thompson, Philos. Mag. **3**, 1174 (1958); A. Arrott and H. Sato, Phys. Rev. **114**, 1420 (1959).

<sup>3</sup>A. T. Aldred, J. Appl. Phys. **37**, 1344 (1966).

<sup>4</sup>A. T. Aldred, J. Phys. C **1**, 1103 (1968).

<sup>5</sup>M. Fallot, Ann. Phys. (Paris) **7**, 420 (1937).

<sup>6</sup>E.g., W. Hume-Rothery and B. R. Coles, Adv. Phys. **3**, 149 (1954).

<sup>7</sup>P. A. Beck, in Proceedings of the International Conference on Magnetism, Nottingham, London, 1964 (Institute of Physics and Physical Society, London, 1964), p. 178; K. P. Gupta, C. H. Cheng, and P. A. Beck, J. Phys. Chem. Solids **25**, 1147 (1964).

<sup>8</sup>C. G. Shull and Y. Yamada, J. Phys. Soc. Jap. Suppl. B-III **17**, 1 (1962).

<sup>9</sup>K. J. Duff and T. P. Das, Phys. Rev. B **3**, 2294 (1971).

<sup>10</sup>G. K. Wertheim, V. Jaccarino, J. H. Wernick, and D. N. E. Buchanan, Phys. Rev. Lett. **12**, 24 (1964).

<sup>11</sup>M. B. Stearns, J. Appl. Phys. **36**, 913 (1965).

<sup>12</sup>M. B. Stearns, Phys. Rev. **147**, 439 (1966).

<sup>13</sup>T. E. Cranshaw, C. E. Johnson, M. S. Ridout, and G. A. Murray, Phys. Lett. **21**, 481 (1966).

<sup>14</sup>L. Brossard, G. A. Fatseas, and J. L. Dormann,

J. Appl. Phys. **42**, 1306 (1971).

<sup>15</sup>B. C. Huguélet, W. C. Harper, C. L. Hummel, C. W. Kimball, and A. P. Paulikas, J. Appl. Phys. **42**, 1312 (1971).

<sup>16</sup>W. C. Harper, C. W. Kimball, and A. T. Aldred, AIP Conf. Proc. **5**, 533 (1971).

<sup>17</sup>L. R. Newkirk and C. C. Tsuei, Phys. Rev. B **4**, 4046 (1971).

<sup>18</sup>G. Trumphy, E. Both, C. Djega-Mariadassou, and P. Lecocq, Phys. Rev. B **2**, 3477 (1970).

<sup>19</sup>I. Vincze and L. Cser, Phys. Status Solidi B **49**, K99 (1972).

<sup>20</sup>I. Vincze and L. Cser, Phys. Status Solidi B **50**, 709 (1972).

<sup>21</sup>K. Yamaguchi, H. Yamamoto, Y. Yamaguchi, and H. Watanabe, J. Phys. Soc. Jap. **33**, 1292 (1972).

<sup>22</sup>I. Vincze and I. A. Campbell, J. Phys. F **3**, 647 (1973).

<sup>23</sup>J. J. Murphy, J. I. Budnick, and S. Skalski, J. Appl. Phys. **39**, 1239 (1968).

<sup>24</sup>E. F. Mendis and L. W. Anderson, Phys. Status Solidi **41**, 375 (1971).

<sup>25</sup>R. H. Dean, R. J. Furley, and R. G. Scurlock, J. Phys. F **1**, 78 (1971).

<sup>26</sup>E. F. Mendis and L. W. Anderson, Phys. Rev. Lett. **19**, 1434 (1967).

<sup>27</sup>G. Gruner, I. Vincze, and L. Cser, Solid State Commun. **10**, 347 (1972).

<sup>28</sup>O. C. Kistner, A. W. Sunyar, and J. B. Swan, Phys.



- Rev. 123, 179 (1961).
- <sup>29</sup>H. S. Moller, *Solid State Commun.* 8, 527 (1970).
- <sup>30</sup>A. E. Balabanov and N. N. Delyagin, *Zh. Eksp. Teor. Fiz.* 57, 1947 (1969) [*Sov. Phys.-JETP* 30, 1054 (1970)].
- <sup>31</sup>E. Both, G. Trumpy, and C. Djega-Mariadassou, *Phys. Lett. A* 35, 27 (1971).
- <sup>32</sup>M. B. Stearns, *Phys. Rev. B* 4, 4081 (1971).
- <sup>33</sup>W. B. Pearson, *Handbook of Lattice Spacings and Structures of Metals and Alloys* (Pergamon, New York, 1958), Vol. 1.
- <sup>34</sup>D. A. Shirley, S. S. Rosenblum, and E. Matthias, *Phys. Rev.* 170, 363 (1968).
- <sup>35</sup>J. Danon, *Rev. Mod. Phys.* 36, 459 (1964).
- <sup>36</sup>G. P. Huffman, F. C. Schwerer, and G. R. Dunmyre, *J. Appl. Phys.* 40, 1487 (1969).
- <sup>37</sup>P. W. Bridgman, *Am. Acad. Sci.* 77, 187 (1949).
- <sup>38</sup>I. A. Campbell, *J. Phys. C* 2, 1338 (1969).
- <sup>39</sup>A. Blandin and I. A. Campbell, *Phys. Rev. Lett.* 31, 51 (1973).
- <sup>40</sup>I. Vincze, *Phys. Rev. B* 7, 54 (1973).
- <sup>41</sup>N. F. Mott, *Adv. Phys.* 13, 325 (1964).